Broadband Linear Power Amplifier for Picocell Basestation Application

Ram Sharma[1], Jagadheswaran Rajendran[1], and Harikrishnan Ramiah[2]
[1] Collaborative Microelectronic Design Excellence Centre (CEDEC), School of Electrical and Electronic Engineering, Engineering Campus, Universiti Sains Malaysia. 14300, Nibong Tebal, Penang, Malaysia
[2] Department of Electrical Engineering, Faculty of Engineering, University of Malaya, 50603 Kuala Lumpur, Malaysia
Email: niteshram@student.usm.my; jaga.rajendran@usm.my; hrkhari@um.edu.my

Abstract —This paper presents the design of a highly linear broadband power amplifier (PA) operating from 200MHz to 3GHz for Long Term Evolution (LTE) pico-cell base station. The monolithic microwave integrated circuit (MMIC) PA is realized with 0.25-μm Enhancement Mode Pseudomorphic High Electron Mobility Transistor (E-pHEMT) process. The broadband PA employs a novel dual feedback technique to achieve the broadband power gain and linearity performance. A low pass input matching network is integrated to suppress the out of band interference. The PA delivers power gain of more than 12dB from 200MHz to 3GHz with peak gain of 20dBm at 450MHz. The achieved OIP3 across the operating frequency is 40dBm with corresponding power added efficiency (PAE) of 45%. The fully matched PA serves to be a good solution for LTE pico-cell base station.

Index Terms—power amplifier, MMIC, pHEMT, LTE, linearity, wideband

I. Introduction

Advanced wireless communication systems such as WCDMA, LTE and Wireless LAN requires low power, high efficiency and high linearity PA. High linearity requirement is crucial in order to increase the immunity of the system against various interferences. Recently linearity performance has been highlighted as the most significant criteria in base station transceiver design in order to achieve higher data rate and support multiple complex modulation techniques such as OFDM and MIMO-OFDM which has a non-constant envelope and sensitive to nonlinear distortions. Furthermore OFDM and MIMO-OFDM signals exhibits high spectral efficiency and large peak to average (PAPR) ratios [1]. The effect of the nonlinearity response in AM and PM on high PAPR modulated signal results in distortion and spectral regrowth which deteriorates the performance of the wireless system in a time varying environment [2]. The degradation of SNR contributed by high PAPR signals can be represented by [3],

$$SNR = 6.02N + 1.76 - p + 10 \log10 [2*SR] \quad (1)$$

where N is the number of bits, p the PAPR and SR the sampling ratio.

Manuscript received February 20, 2017; revised July 13, 2017.
Corresponding author email: jaga.rajendran@usm.my
doi:10.12720/jcm.12.7.419-425

Efficiency improvement techniques such as Doherty [4], Envelope Tracking [5], EE&R [6] and Switch mode PA [7] are gaining wide attention lately. Doherty PA exhibits high efficiency across wide range of output power as compared to class B PA by utilizing the load modulation technique [8]. The Doherty PA was first introduced by [9] and consists of carrier and peaking transistors. Optimum efficiency is achieved when both transistors modulate concurrently. However, phase distortion is eminent when both transistors are operating simultaneously at high peak power and backed-off power levels due to Miller phenomenon [10].

Distributed amplifier is suitable for wideband design and has demonstrated exceptional bandwidth [11]. However, low efficiency performance and large form factor design has made this topology unattractive for advance wireless systems. Recently, switch mode amplifier topology has demonstrated high efficiency of more than 70% [12]. The drawback of this circuit topology is its highly sensitive to the output impedance thus resulting in limited bandwidth [13].

CMOS PA is gaining attention lately and has shown high potential of system level integration and single chip solution [14]. However, low efficiency and power limitation is eminent due to the high substrate loss and low breakdown voltage of CMOS process [15]. On the other hand, wide bandgap technologies such as GaN which has high breakdown voltage, high electron mobility and excellent thermal conductivity capability has shown promising adoption for wireless basestation applications [16]. This provides component manufacturers with option to design with GaN technology which has the benefits of high power density, high linearity and low noise performances across wide operating frequencies [17]. However, wide acceptance in industry is still questionable with high cost, low yield and inferior reliability of this new semiconductor technology [18].

GaAs E-pHEMT technology has the advantage of providing low noise and minimum trade-off between linearity and efficiency which is desired in modern wireless communication system, particularly beyond 2GHz as compared to Si-BJT, SiGe HBT and InGaP HBT technology [19], [20]. In order to meet the linearity performance for PA designed in the above mentioned

process, complex techniques such as the pre-distortion is utilized [21]. However, the trade-off is the broadband performance. Fig. 1 illustrates the transceiver architecture of a LTE pico-cell basestation [22].

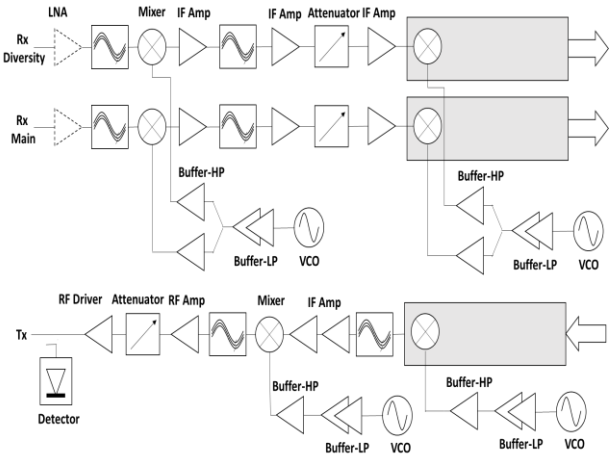

Fig. 1. LTE Pico-cell transceiver architecture.

Referring to the figure above, a high OIP3 and broadband PA is required to reduce the number of the amplifier stages in the transmitter chain. This paper demonstrates for the first time the design of a highly linear broadband PA with 0.25-µm E-pHEMT process. The broadband PA features an integrated dual feedback network to achieve a broadband linearity performance. An integrated low pass filter circuit which has an impedance close to 50 ohm has been implemented at the input of the PA to reject the out of band interference, thus eradicating the need of an external attenuator as depicted in Fig. 1.

This paper is organized as follows. Section II describes the design methodology of the broadband PA followed by the validation results in Section III. Section IV summarizes the conclusion.

II. Design Methodology

The design goal of this PA is to achieve a broadband operating frequency from 200MHz to 3GHz with minimum OIP3 of 40dBm, 0.5W linear output power while achieving less than 100mA DC current consumption with supply voltage headroom of 5V. Before embarking in to the design of the PA, device or technology selection and transistor configuration is an important aspect to be carefully considered.

A. Device Selection

GaAs E-pHEMT process has been chosen since it has demonstrated wideband characteristics of high efficiency and linearity and is widely used in base-station development lately [23]. E-pHEMT technology is attractive for gain block/driver amplifiers because it provides highly linear performance across a wide bandwidth which is useful in next generation communication systems. In addition, GaAS Enhancement-mode pHEMT (E-pHEMT) technology combines advantages of both HBT and depletion-mode pHEMT (D-pHEMT) technologies in a single process [23]. Similar to HBT, it allows single supply operation and does not require drain switch to turn the PA completely off as well as high efficiency similar to a D-pHEMT process. Furthermore, GaAs E-pHEMT has high breakdown tolerance and ability to with stand high temperature variations.

This advantages is key to maintain the overall system performance in advance and high level integrated infrastructure systems. With this, pre-amplifier limiter circuitry is not required and this helps to improve the overall system SINAD [24]. Table I summarizes the DC characteristics of the GaAS Enhancement-mode pHEMT (E-HEMT) transistor.

TABLE I: DC CHARACTERISTICS OF GAAS (E-PHEMT) TRANSISTOR

Parameter	*Mean*
G_m (mS/mm)	580
V_{gs} @ peak Gm (V)	0.7
I_{ds} @ peak Gm (mA/mm)	171
I_{max} (mA/mm) @ $V_{gs} = V_{to}$	331
BV_{gd} @ 1mA/mm (V)	-17
V_{to} @ 1mA/mm (V)	0.97
V_{th} @ 1mA/mm (V)	0.25

B. Power Amplifier Configuration

Three most common FET configurations for PA designs are: Common Source (CS), Common Gate (CG) and Common Drain (CD) [25]. The common source configuration exhibits highest power gain and is the most suitable configuration for wideband PA design. Table II compares the characteristic of the basic FET configurations.

TABLE II: CHARACTERISTICS OF FET CONFIGURATIONS

Characteristics	Common Source	Common Gate	Common Drain
Voltage Gain, A_V	$-g_m \frac{R_L R_{ds}}{R_L + R_{ds}}$	$g_m R_L$	$\frac{g_m R_L}{1+g_m R_L} < 1$
C_{in}	$C_{gs}+(1-A_V)C_{gd}$	$C_{gs}+(1-A_V)C_{gd}$	$C_{gs}+(1-A_V)C_{gd}$
Input Impedance, Z_{in}	High	$\frac{R_{ds}+R_L}{g_m R_{ds}+1} \cong \frac{1}{g_m}$	High
Output Impedance, Z_{out}	R_{ds}	$R_{ds}+(g_m R_{ds}+1)R_L$	$\fr\frac{R_{ds}}{g_m R_{ds}+1} \| \cong \frac{1}{g_m}$
Reverse Isolation	Best	Good	Poor

PA circuits are classified into different classes depending on the DC biasing of the transistor. For high linearity and acceptable efficiency for wideband frequency operation, generally class A, AB and C are applied [26]. Fig. 2 illustrates the simplified circuit elements of a pHEMT PA. The high frequency AC input signal is injected via the gate of the FET through C_{in} and amplified as output signal to the load through C_{out}. The inductors L_{in} and L_{out} functions as high impedance RF chokes and prevents the signals from coupling to the DC supplies. Meanwhile, C_{in} and C_{out} prevents the DC currents from passing through the signal source and load.

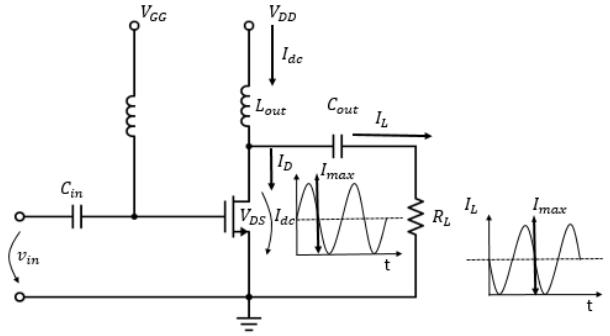

Fig. 2. pHEMT amplifier with high frequency AC current flow.

The optimum load line resistance for maximum power transfer is given as [27]:

$$R_L = \frac{V_m - V_k}{I_{\max}} \tag{2}$$

where V_k is the knee voltage, V_m is equal to ($2V_{DD}$ - V_k), I_{max} is the maximum drain current when V_{gs} is equals to zero. The output power increases as V_m increases. Hence, the maximum output power is given as:

$$P_{out,\max} = \frac{I_{\max}(V_{m.\max} - V_k)}{8} \tag{3}$$

where ($V_{m,max}$ - V_k)/2 is the drain–source voltage for maximum output power.

The power added efficiency of a PA is defined by

$$PAE \approx \frac{1}{2}\frac{V_{m.\max} - V_k}{V_{m.\max} + V_k} X100\% \tag{4}$$

From (4), the theoretical limit of PAE for a class A amplifier is 50%. The total power dissipated in the transistor is given in equation (5):

$$P_{FET} = \frac{1}{8} I_{\max} V_m + \frac{3}{8} I_{\max} V_m \tag{5}$$

C. Device Selection

pHEMT amplifier linearity has been widely researched where various techniques are proposed to enhance the linearity especially in nonlinear weakly region [28]. Fig. 3 depicts the nonlinear pHEMT circuit model with extrinsic linear elements [29].

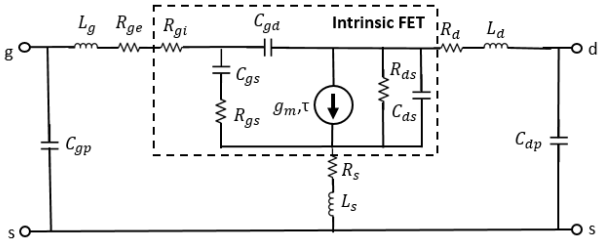

Fig. 3. Nonlinear pHEMT circuit model with extrinsic linear elements.

The RF transistor transconductance g_m is defined as the ratio of drain current $I_{ds}(\omega_o)$ to the gate voltage $V_{ds}(\omega_o)$ when the drain is AC shorted [29] as given in (6).

$$G_m = \frac{I_{ds}(\omega_O)}{V_{gs}(\omega_O)} \tag{6}$$

The nonlinear input capacitance C_{gs} and the nonlinear gate drain capacitance C_{gd} causes AM/AM and AM/PM distortions. The AM/AM distortion is minimal at lower frequency, however at higher frequencies the impact is further aggravated by the nonlinear input capacitance and source mismatch [30]. Ideally, the AM/PM characteristics of the PA is effected by the device transconductance and interaction of knee voltage [31]. However, with suitable input matching network and by incorporating distortion compensation techniques, the AM/PM nonlinearities can be further minimized [32]. The nonlinear distortion is improved through effective cancellation as shown in Fig. 4. The operation theory of memoryless distortion can be modelled using power series [33],

$$y = a_1.x + a_2.x^2 + a_3.x^3 \tag{7}$$

where a_1 to a_3 are the nonlinearity coefficients. These nonlinear components generate new spectral components as shown in Fig. 4.

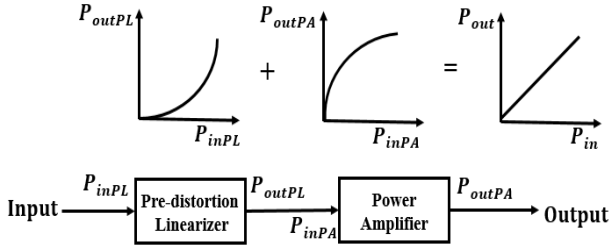

Fig. 4. Non Linear distortion analysis

Volterra series extends the prediction of conventional power series equation to calculate the nonlinear amplitude and phase effects concurrently [34]. The distortions are modelled as depicted in Fig. 5 whereby the nonlinear current sources at the gate and drain are defined.

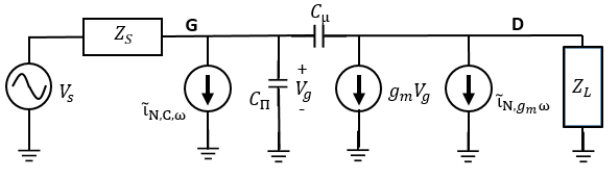

Fig. 5. Nonlinear amplifier current model [28].

In order to obtain broadband gain and low power consumption simultaneously, a dual feedback technique has been employed in this work. The resistive feedback extends the bandwidth of the PA by suppressing the lower frequency gain and improves the gain flatness across wider bandwidth [35]. The dual feedback network consist of a shunt network between the drain and gate of the MESFET Q1 and also a series network connected to the source of the Q1 as illustrated in Fig. 6.

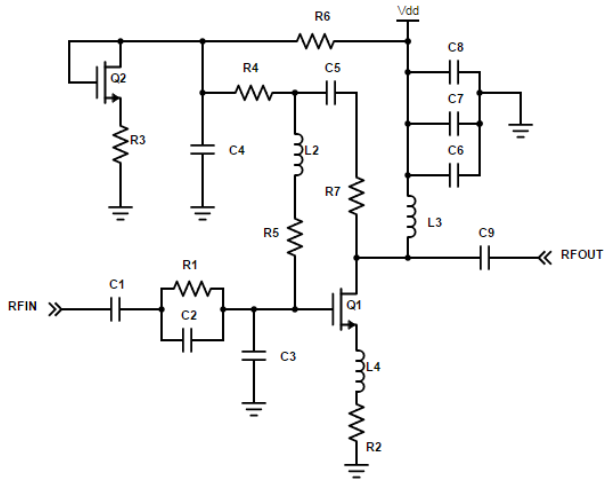

Fig. 6. Schematic of the broadband linear PA

The shunt feedback network is consist of resistor R_5, R_7, inductor L_2 and capacitor C_5 whereas L_4 and R_2 forms the series feedback. Through these networks a broadband linear power gain performance is achieved for the PA. The relationship between the dual feedback networks to the linear power gain S_{21} is given as:

$$S_{21} = \frac{1}{D}\left(\frac{-2g_m Z_0}{1+g_m[R_2+j\omega L_4]} + \frac{2Z_0}{(R_5+R_7)-j\omega[C_5-L_2]}\right)$$
$$\text{where} \qquad (8)$$
$$D = 1+\frac{2Z_0}{(R_5+R_7)-j\omega[C_5-L_2]} + \frac{g_m Z_0^2}{\left[((R_5+R_7)-j\omega[C_5-L_2])(1+g_m(R_2+j\omega L_4))\right]}$$

where Z_0 in equation 1 represents the output impedance of Q1.

The PA is biased at class-A with a positive gate voltage provided by a current mirror biasing circuit which consist of MESFET Q2, R_3, R_4, R_6 and C_4. R_6 forms a constant current source for Q2, thus providing a stable gate voltage for the PA. Hence the PA is robust against drain supply voltage variation. On the other hand, a low pass filter has been integrated at the input of Q1 which is represented by C_1, C_2, C_3 and R_1. This network rejects the out of band interference.

III. Validation Results

The simulated S-parameters performance of the proposed broadband LTE PA with supply headroom of 5.0V is shown in Fig. 7. S_{11} and S_{22} results indicates the amplifier is matched close to 50Ω across from 200MHz to 3GHz, resulting an operating bandwidth of 2.8GHz. The broadband PA achieves minimum power gain of 13dB across the operating bandwidth. The maximum power gain is 20.5dB at 200 MHz.

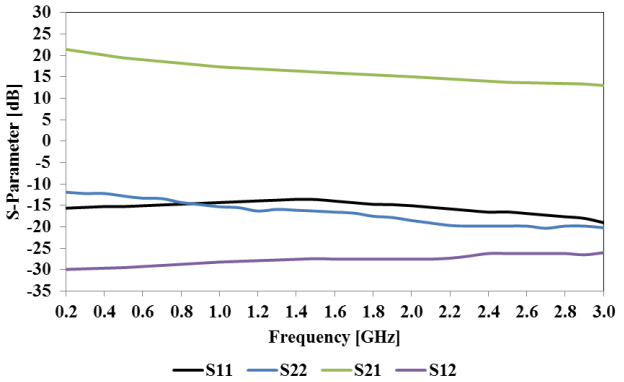

Fig. 7. Simulated S-Parameter performance of Broadband PA, covering an operating bandwidth of 2.8GHz

Stability K-factor indicates that the PA is unconditionally stable up to 20GHz as illustrated in Fig. 8.

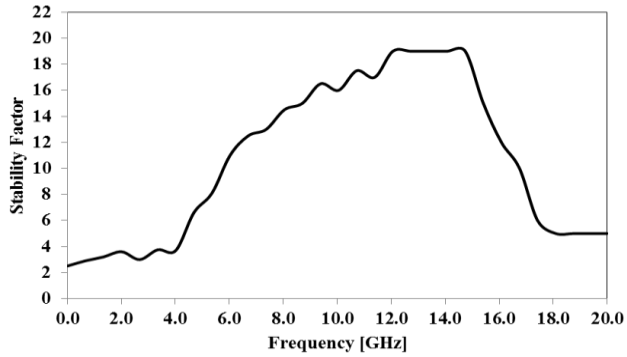

Fig. 8. Stability K-Factor of Broadband PA from DC to 20GHz.

Fig. 9 depicts the 1dB compressed output power (P1dB) across operating frequency with current consumption of 95mA. In average the achieved P1dB is 24dBm.

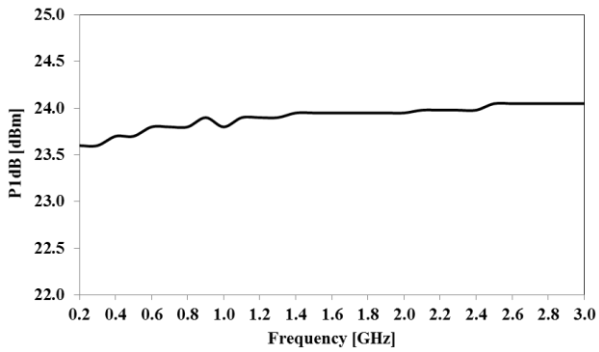

Fig. 9. Simulated P1dB result.

The linearity performance of the PA in terms of OIP3 parameter is illustrated in Fig. 10. The OIP3 is simulated at 6dB back-off output power from the P1dB with dual signal tone with 10MHz spacing as the input signal.

Referring to Fig. 10, it can be observed that an average broadband OIP3 of 40dBm is achieved from 200MHz to 3GHz. Fig. 11 shows the resultant power added efficiency (PAE) of the PA from 200MHz to 3GHz. A minimum

PAE of 45% is achieved across the mentioned operating frequency.

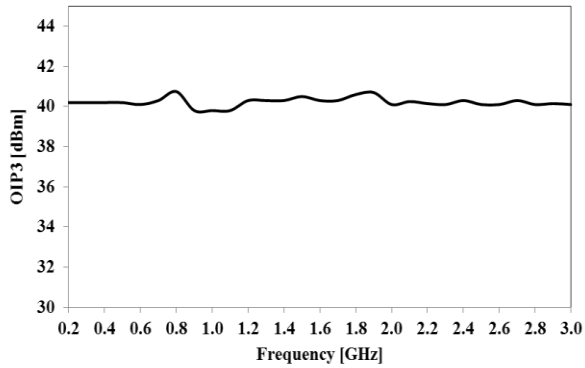

Fig. 10. OIP3 across frequency of Broadband PA

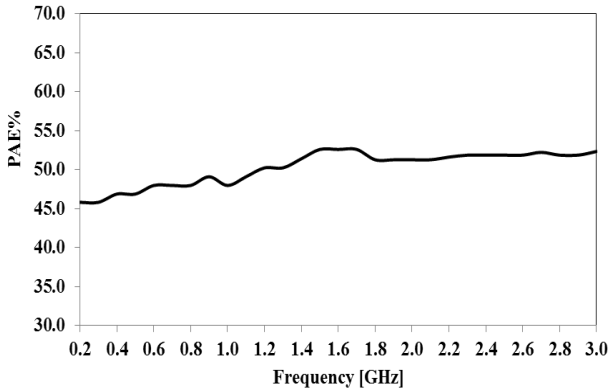

Fig. 11. PAE performance of the broadband PA

In Table III, the performance comparison with recently reported works is presented.

TABLE III: PERFORMANCE COMPARISON WITH RECENT PUBLICATIONS

Reference	Freq (GHz)	Vdd (V)	Gain (dB)	OIP3 (dBm)	P1dB (dBm)	ACLR(dBc)	PAE%
[36]	0.5 – 2.0	40.0	20.0	47	35	-	15.8
[37]	0.1-1.0	5.0	20.2	34.2	21.8	-	33.6
[38]	0.7- 2.0	1.2	21.2	13.5	3.01	-	-
[39]	0.82-0.92	3.6	26.6	-	26.0	-30.2	23-25.3
[40]	1.95	3.4	28.5	-	26.0	-32.5	26.6
This work	0.2-3.0	5.0	20.5-13.0	40.0	24.0	-	>45.0

IV. CONCLUSION

In this paper, the design of a highly linear broadband PA has been presented. This PA consist of a novel dual feedback network which delivers a broadband linear output power while maintaining an unconditional stability performance. An integrated 50Ω low pass filter is integrated at the input of the PA which prevents the amplification of out band interference and noise which originates from the preceding stage. The validation results highlights the potential application of the proposed PA in multi-band wireless LTE pico-cell base station.

ACKNOWLEDGMENT

Our thanks to CEDEC Universiti Sains Malaysia for supporting this research work.

REFERENCES

[1] C. H. U. Baek, G. W. Park, and J. W. Jung, "An efficient receiver structure for faster-than-nyquist signal in MIMO system," *Journal of Communications*, vol. 12, no. 5, pp. 285-290, 2017.

[2] Z. Hailu, K. Langat, and C. Maina, "Stratified ACO-OFDM modulation for simultaneous transmission of multiple frames both on even and odd subcarriers," *Journal of Communications*, vol. 12, no. 5, pp. 261-270, 2017.

[3] P. Cruz and N. B. Carvalho, "PAPR evaluation in multi-mode SDR transceivers," in *Proc. 38th European Microwave Conference*, New York, 2008, pp. 1354 - 1357.

[4] H. Oh, H. Kang, H. Lee, *et al*., "Doherty power amplifier based on the fundamental current ratio for asymmetric cells," *IEEE Transactions on Microwave Theory and Techniques*, pp. 1-8, 25 May 2017.

[5] J. Kim, D. Kim, Y. Cho, D. Kang, B. Park, K. Moon, S. Koo, and B. Kim, "Highly efficient RF transmitter over broad average power range using multilevel envelope-tracking power amplifier," *IEEE Transactions on Circuits and Systems I: Regular Papers*, vol. 62, no. 6, pp. 1648 - 1657, June 2015.

[6] X. Liu, H. Zhang, M. Zhao, X. Chen, P. K. T. Mok, and H. C. Luong, "2.4 A 2.4V 23.9dBm 35.7%-PAE -32.1dBc-ACLR LTE-20MHz envelope-shaping-and-tracking system with a multiloop-controlled AC-coupling supply modulator and a mode-switching PA," presented at the IEEE International Solid-State Circuits Conference (ISSCC), Feb. 5-9, 2017.

[7] C. Zhi and Y. H. Zh., "A new adaptive delay method for wideband wireless Kahn's RF power amplifiers," *IEEE Transactions on Consumer Electronics*, vol. 52, pp. 962-965, Aug. 2006.

[8] J. Kim, B. Fehri, S. Boumaiza, and J. Wood, "Power efficiency and linearity enhancement using optimized asymmetrical Doherty power amplifiers," *IEEE Trans. Microw. Theory Tech.*, vol. 59, no. 2, pp. 425–434, Feb. 2011.

[9] W. H. Doherty, "A new high efficiency power amplifier for modulated waves," *Proc. Inst. Radio Eng.*, vol. 24, no. 9, pp. 1163–1182, Sep. 1936.

[10] S. Chen and Q. Xue, "Optimized load modulation network for Doherty power amplifier performance enhancement," *IEEE Trans. Microw. Theory Tech.*, vol. 60, no. 11, pp. 3474–3481, Nov. 2012.

[11] P. Dennler, S. Maroldt, R. Quay, and O. Ambacher, "Monolithic three-stage 6–18GHz high power amplifier

with distributed interstage in GaN technology," presented at the Microwave Integrated Circuits Conference (EuMIC), 2015 10th European, Sept. 7-8, 2015.

[12] J. Hur, O. Lee, C. H. Lee, K. Lim, and J. Laskar, "A multi-level and multi-band class-D CMOS power amplifier for the LINC system in the cognitive radio application," *IEEE Microwave and Wireless Components Letters*, vol. 20, pp. 352-354, June 2010.

[13] U. R. Jagadheswaran, H. Ramiah, P. I. Mak, R. P. Martins, "A 2um InGaP/GaAs Class- J power amplifier for multi-band LTE achieving 35.8-dB gain, 40.5% to 55.8% PAE and 28-dBm linear output power," *IEEE Transactions on Microwave Theory and Techniques*, vol. 64, no. 1, January 2016.

[14] B. Kim, S. Jin, B. Park, Y. Cho, C. X. Zhao, and K. Moon, "Advanced design of differential CMOS PA," presented at the IEEE Topical Conference Power Amplifiers for Wireless and Radio Applications (PAWR), Jan. 19-23, 2014.

[15] Y. H. Qi, R. L. He, and Z. Shen, "A 32 GHz low-power low-phase-noise VCO implemented in SiGe BiCMOS technology," *Journal of Communications*, vol. 12, no. 2, pp. 98-104, 2017.

[16] J. J. M. Rubio, V. Camarchia, R. Quaglia, E. F. A. Malaver, and M. Pirola, "A 0.6–3.8 GHz GaN power amplifier designed through a simple strategy," *IEEE Microwave and Wireless Components Letters*, vol. 26, pp. 446-448, June 2016.

[17] R. Giofré and P. Colantonio, "A high efficiency and low distortion 6 W GaN MMIC doherty amplifier for 7 GHz radio links," *IEEE Microwave and Wireless Components Letters*, vol. 27, pp. 70-72, Jan. 2017.

[18] S. Cha, Y. H. Chung, M. Wojtowicz, *et al*., "Wideband ALGaN/GaN HEMT low noise amplifier for highly survivable receiver electronics," in *IEEE MTT-S Dig*., Fort Worth, TX, Jun. 2004, pp. 829–832.

[19] J. Jung, G. Lee, and J. I. Song, "A SiGe HBT power amplifier with integrated mode control switches for LTE applications," in *Proc. Radio and Wireless Symposium (RWS)*, Jan. 20-23, 2013, pp. 238-240.

[20] C. K. Lin, S. J. Li, S. H. Tsai, *et al*., "The monolithic integration of InGaAs pHEMT and InGaP HBT technology for single-chip WiMAX RF front-end module," in *Proc. 54th International Midwest Symposium on Circuits and Systems*, Aug. 7-10, 2011, pp. 1-4.

[21] W. C. Hua, H. H. Lai, P. T. Lin, *et al*., "High-linearity and temperature-insensitive 2.4 GHz SiGe power amplifier with dynamic-bias control," in *Proc. IEEE Asia-Pacific Conference Circuits and Systems*, Dec. 6-9, 2004, pp. 609-612.

[22] C. Lin and Y. C. Hsu, "Single-chip dual-band WLAN power amplifier using InGaP/GaAs HBT," in *Proc. Microwave Conference*, European, 4-6 Oct. 2005, pp. 1438-1441.

[23] K. W. Kobayashi, "High linearity-wideband pHEMT Darlington amplifier with +40 dBm IP3," in *Proc. Microwave Conference*, Asia-Pacific, Dec. 12-15, 2006, pp. 1035-1038.

[24] M. V. Aust, A. K. Sharma, Y. C. Chen, and M. Wojtowicz, "Wideband dual-gate GaN HEMT low noise amplifier for front-end receiver electronics," presented at the 2006 IEEE Compound Semiconductor Integrated Circuit Symposium, 12-15 Nov. 2006, pp. 89-92.

[25] I. Bahl, *Fundamentals of RF and Microwave Transistor Amplifiers*, Hoboken, New Jersey: John Wiley & Sons, 2009, p. 71.

[26] S. Cripps, *RF Power Amplifiers for Wireless Communications*, ser. Artech House Microwave Library, Norwood, MA, USA: Artech, 2006, pp. 47-53.

[27] F. Schwierz and J. J. Liou, *Modern Microwave Transistors: Theory, Design, and Performance*, Hoboken, New Jersey: John Wiley & Sons, 2003, pp. 205-208.

[28] A. Kheirkhahi, J. J. Yan, P. M. Asbeck, and L. E. Larson, "RF power amplifier efficiency enhancement by envelope injection and termination for mobile terminal applications," *IEEE Transactions on Microwave Theory and Techniques*, vol. 61, pp. 878-889, Feb. 2013.

[29] A. Grebennikov, *RF and Microwave Power Amplifier Design*, McGraw-Hill Companies, 2009, pp. 57-58.

[30] J. X. Deng, P. S. Gudem, L. E. Larson, D. F. Kimball, and P. M. Asbeck, "A SiGe PA with dual dynamic bias control and memoryless digital predistortion for WCDMA handset applications," *IEEE Journal of Solid-State Circuits*, vol. 41, pp. 1210-1221, May 2006.

[31] J. X. Deng, P. S. Gudem, L. E. Larson, D. F. Kimball, and P. M. Asbeck, "A SiGe PA with dual dynamic bias control and memoryless digital predistortion for WCDMA handset applications," *IEEE Journal of Solid-State Circuits*, vol. 41, pp. 1210-1221, May 2006.

[32] P. Draxler, J. Deng, D. Kimball, I. Langmore, and P. Asbeck, "Memory effect evaluation and predistortion of power amplifiers," in *Proc. IEEE MTT-S Int. Microw. Symp. Dig.*, Jun. 2005, pp. 1549–1552.

[33] V. Leung, J. Deng, P. Gudem, and L. Larson, "Analysis of envelope signal injection for improvement of RF amplifier intermodulation distortion," *IEEE J. Solid-State Circuits*, vol. 40, no. 9, pp. 1888–1894, Sep. 2005.

[34] J. Vuolevi and T. Rahkonen, *Distortion in RF Power Amplifiers*, MA: Artech House, 2003, pp. 71-118.

[35] K. W. Kobayashi, Y. C. Chen, I. Smorchkova, and B. Heying, "A cool, sub-0.2 dB noise figure GaN HEMT power amplifier with 2-watt output power," *IEEE Journal of Solid-State Circuits*, vol. 44, pp. 2648-2654, Oct. 2009.

[36] K. W. Kobayashi, "An 8-W 250-MHz to 3-GHz decade-bandwidth low-noise GaN MMIC feedback amplifier with > +51-dBm OIP3," *IEEE Journal of Solid-State Circuits*, vol. 47, no. 10, October 2012.

[37] K. W. Kobayashi, "Improved efficiency, IP3-Bandwidth and robustness of a microwave darlington amplifier using 0.5um ED PHEMT and a new circuit topology," in *Proc. Compound Semiconductor Integrated Circuit Symposium*, 2005.

[38] Z. Pan, C. Qin, Z. C. Ye, and Y. Wang, "A Low power inductorless wideband LNA with GM enhancement and noise cancellation," *IEEE Microwave And Wireless Components Letters*, vol. 27, no. 1, January 2017.

[39] G. Y. Lee, J. H. Jung, and J. I. Song, "A SiGe BiCMOS power amplifier using a lumped element-based impedance tuner," *IEEE Microwave and Wireless Components Letters*, vol. 26, no. 1, pp. 58-60, 2016.
[40] G. Lee, J. Jung, and J. Song, "A 26 dBm output power SiGe power amplifier for mobile LTE applications," in *Proc. IEEE Radio Wireless Symp*., Jan. 2013, pp. 232-234.

Ram Sharma Nitesh was born in Kedah, Malaysia. He received the B.Eng degree (Hons) from the University Teknologi Malaysia, Johor, Malaysia, in 2001, the M.Eng degree in Electronics from University Sains Malaysia, Penang, Malaysia, in 2010.Currently he working towards his Ph.D. degree in RF integrated circuit (IC) design at Collaborative Microelectronic Design Excellence Centre (CEDEC) Universiti Sains Malaysia, Penang. His research interest includes RFIC, MMIC and Antenna design include spectral estimation, array signal processing, and information theory.

Jagadheswaran Rajendran was born in Pulau Pinang, Malaysia. He received his B.Eng degree (Hons) from Universiti Sains Malaysia, Pulau Pinang, Malaysia, in 2004, the M.Eng degree in Telecommunications from Malaysia Multimedia University, Cyberjaya, Malaysia, in 2011, and the Ph.D. degree in Radio Frequency Integrated Circuit (RFIC) design from the University of Malaya, Kuala Lumpur, Malaysia, in 2015. He is currently a Senior Lecturer at Collaborative Microelectronic Design Excellence Centre (CEDEC) and School of Electronic Engineering, Universiti Sains Malaysia. His research interest is RFIC design, analog IC design and RF system design for mobile wireless communications which has resulted several technical publications. He holds one US patent and one International patent. Dr Jagadheswaran was the recipient of the IEEE Circuit and System Outstanding Doctoral Dissertation Award in 2015. He is a Senior Member of IEEE and currently serves as the Vice Chairman of IEEE ED/MTT/SSC Penang Chapter.

Harikrishnan Ramiah is currently an Associate Professor at Department of Electrical Engineering, University of Malaya, working in the area of RFIC design. He received his B.Eng(Hons), MSc and PhD degrees in Electrical and Electronic Engineering, in the field of Analog and Digital IC design from Universiti Sains Malaysia in 2000, 2003 and 2008 respectively. He was with Intel Technology, Sdn. Bhd attached in power gating solution of 45 nm process. In the year 2003, he was with SiresLabs Sdn. Bhd, CyberJaya, Malaysia working on 10Gbps SONET/SDH Transceiver solution. At the year 2002 he was attached to Intel Technology, Sdn. Bhd performing high frequency signal integrity analysis for high speed digital data transmission and developing Matlab spread sheet for Eye diagram generation, to evaluate signal response for FCBGA and FCMMAP packages. Harikrishnan was the recipient of Intel Fellowship Grant Award, 2000-2008. He is a Chartered Engineer of Institute of Electrical Technology (IET) and also a Professional Engineer registered under the Board of Engineers, Malaysia. He is a member of The Institute of Electronics, Information and Communication Engineers (IEICE) and an elevated Senior Member of the Institute of Electrical and Electronics Engineer (IEEE). His research work has resulted in several technical publications. His main research interest includes Analog Integrated Circuit Design, RFIC Design, VLSI system and RF Energy Harvesting Power Management Module Design.